^{13}C Magnetic Resonance Signal Density and Relaxation Times of Crude Oils

Naser Ansaribaranghar[1,2], *Mohammad Sadegh* Zamiri[1], *Laura* Romero-Zerón[2], *Florea* Marica[1], *Andres* Ramirez Aguilera[1], *Michael J.* Dick[4], *Derrick* Green[4], *Benjamin* Nicot[3], *and Bruce J.* Balcom[1,*]

[1]UNB MRI Centre, Department of Physics, University of New Brunswick, Fredericton, New Brunswick E3B 5A3, Canada
[2]Department of Chemical Engineering, University of New Brunswick, Fredericton, New Brunswick E3B 5A3, Canada
[3]TotalEnergies, Avenue Larribau, 64000 Pau, France
[4]Green Imaging Technologies, Fredericton, New Brunswick E3A 8V2, Canada

Abstract. Accurate determination of fluid saturations in core plugs is crucial in the petroleum industry. Conventional laboratory methods rely on fluid extraction. Therefore, they disrupt fluid saturation and are time-consuming. In contrast, Magnetic Resonance (MR) is a non-invasive tool that requires minimal sample preparation, and samples remain intact for the measurement. While ^{1}H MR is widely used for core analysis, overlapping of oil and water signal components becomes a major issue for quantification of fluid saturations. Existing techniques to resolve signal have limitations, but a promising new approach involves using ^{13}C MR data to determine fluid saturations. Although ^{13}C MR results in accurate saturation determinations, but similar to ^{1}H MR, this method requires a reference sample to convert the ^{13}C signal to quantity of oil. In this study, we investigated the ^{13}C and ^{1}H MR signal per volume and signal per mass for various crude oils from different regions of the world with API ranging from 25 to 50. These investigations aimed to determine whether the ^{13}C signal per volume or ^{13}C signal per mass of different crude oils falls within a prescribed range. This permits eliminating the need for a special reference sample in determining oil saturations from core plugs using ^{13}C and ^{1}H MR experiments. Results show that the ^{13}C and ^{1}H signal per volume of the crude oils tested in this study shows a variation with a confidence of ~ 5% and 4% respectively. This corresponds to a maximum relative error of 5% in saturation measurements. Linear trends were observed between the above ratios and density of crude oils. This suggests that having only the density of a crude oil is enough to obtain accurate volumes and saturations. The application of this method will greatly enhance the precision of determining fluid saturation in core plugs through MR techniques, particularly in cases where the reference oil is not accessible. Furthermore, we measured ^{13}C and ^{1}H MR relaxation times and their correlations (T_1, T_2, and T_1-T_2) for these crude oils. For some crude oils similar trends and ranges were observed for ^{1}H and ^{13}C T_1-T_2 relaxation correlations, suggesting merit in further investigation.

1 Introduction

Saturation plays a crucial role for estimating the volume of oil and gas reserves [1]. The petroleum industry relies on three standard techniques to determine water and oil saturations. These methods include resistivity logging [2–6], capillary pressure saturation modeling [6,7], and direct measurement of water content in preserved core plug samples using the Dean-Stark distillation extraction method [8–10].

The determination of average water saturation in preserved samples involves extracting water using hot toluene vapors and collecting the extracted water. The volume of collected water is then measured for quantitative estimation of saturation. However, this process is prone to errors due to factors like extraction efficiency, losses during collection, and volume measurement inaccuracies. Careful experimental technique and rigorous quality control are essential to minimize errors and ensure reliable results [8,9]. Additionally, this method is time-consuming and involves the use of toluene, a hazardous organic solvent [11]. Therefore, there is a need for non-invasive, fast, and accurate methods for saturation determination.

Magnetic resonance (MR) provides a robust set of techniques for investigating fluids that reside in the reservoir rock at the laboratory and wellbore scale. Typical MR core analysis measurement involves obtaining a distribution of transverse relaxation lifetimes, T_2, using the well-known Carr-Purcell-Meiboom-Gill (CPMG) measurement [12,13]. In practical scenarios, it is common to observe significant overlap of ^{1}H MR signal in the T_2 distributions of realistic samples [1,14–21]. In previous papers by the authors [22,23], we showed a novel approach using ^{13}C and ^{1}H to determine the water and oil content in a rock sample by employing the naturally

---

[*] Corresponding author: bjb@unb.ca

occurring ^{13}C in the hydrocarbon phase. It was shown that initial knowledge of pore volume removes the necessity of having ^{1}H MR, and only ^{13}C MR is sufficient to obtain oil and water saturations. Although the results were promising, like every ^{1}H MR measurement, having reference samples of the saturating oil was necessary to convert signal to volumes.

Building on this groundwork, this work aimed to further the application of ^{13}C MR by focusing on its signal intensity variations across different crude oils, exploring how ^{13}C content of oils differ from each other. Understanding in what range the ^{13}C signal intensity per volume and signal intensity per mass changes would allow studying unknown core plug samples saturated with unknown oil saturated samples and determining the oil saturations without direct reference samples. Using this approach reference samples are not required, and oil saturation in the core plug can be estimated using a generic crude oil or synthetic oil as the reference sample.

For this purpose, decane and eight crude oils from different continents with different densities were studied. Results show that ^{13}C signal intensities per volume differ in an acceptable range. It also shows that there is a relationship between density of oil and the ^{13}C signal intensities. To see how this idea works in core plugs, 5 Bentheimer core plugs saturated with crude oil and brine were tested. The oil content of the samples was known from Special Core Analysis (SCAL). To obtain the oil content from ^{13}C MR measurements, the signal per volume of dodecane was used as a reference sample.

The insights gained from these investigations underscore the potential of ^{13}C MR to not only match but potentially exceed the performance of traditional methods like Dean-Stark analysis in terms of speed, safety, and efficacy.

2 Materials and methods

2.1 Rock and fluid properties

Two sets of samples were used: Set 1 consisted of Decane and eight different crude oils in vials to determine the signal density of different crude oils. Set 2 included five core plug samples saturated with brine and an unknown crude oil with known fluid saturations that were tested to evaluate the accuracy of oil saturation measurements using ^{13}C MR signals, with the aim of assessing the potential error in saturation measurements when a different oil is used for calibration and eventually the volume calculation.

Table 1 shows the volume, mass, and density of the crude oils that have been used in set 1 samples. The crude oils are from different continents and have API ranging from 25 to 50. Table 2 shows the properties of the core plugs used in sample set 2.

Table 1. Crude oil properties.

Sample Id	Mass [g]	Volume [ml]	Density [g/ml]
Oil1, (Decane)	3.06	3.46	0.73
Oil2	3.93	4.47	0.86
Oil3	3.86	4.50	0.83
Oil4	4.21	4.71	0.89
Oil5	3.87	4.63	0.81
Oil6	3.74	4.28	0.86
Oil7	4.08	4.53	0.88
Oil8	3.63	4.25	0.8
Oil9	3.35	4.26	0.77

Table 2. Core plug properties.

Core Id	Porosity [v/v]	Pore volume [ml]	Oil saturation [v/v]
Be1	0.246	14.03	0.098
Be2	0.244	13.81	0.115
Be3	0.248	14.22	0.105
Be4	0.249	14.20	0.177
Be5	0.243	13.83	0.161

2.2 MR measurements

^{13}C and ^{1}H MR experiments were undertaken to obtain T_2, and T_1-T_2 relaxation correlations. Two-dimensional T_1-T_2 relaxation correlations were obtained using the Inversion-Recovery-CPMG sequence. Details of the T_1-T_2 measurement can be found elsewhere [24–26]. The IR-CPMG pulse sequence, Figure 1, begins with a 180° pulse, then after a recovery time t_{int}, a 90° pulse is applied followed by a series of 180° pulses to acquire a CPMG echo train. The signal equation is described by:

$$S(t, t_{int}) = \iint dT_1 dT_2 f(T_1, T_2)(1 - 2\exp\{-t_{int}/T_1\})\exp\{-t/T_2\} \quad (1)$$

where $f(T_1, T_2)$ is the T_1-T_2 distribution function, t is the cumulative echo time starting at the 90° pulse while t_{int} is the recovery time between the inverting 180° pulse and the subsequent 90° pulse of the CPMG measurement. Data analysis involves a 2D Laplace inversion to extract $f(T_1, T_2)$ from the measured set of echo amplitudes $S(t, t_{int})$.

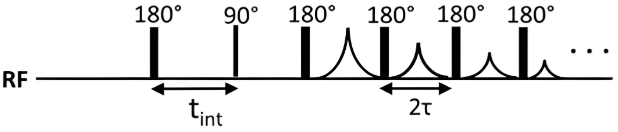

Fig. 1. IR-CPMG pulse sequence [27].

The 90° and 180° rf pulse durations for ^{13}C measurements were t_{90}= 28.2 μs and t_{180} = 56.6 μs, respectively. T_2 relaxation times were determined using the standard CPMG experiment [30,31]. In ^{13}C measurements the temporal separation of spin echoes was t_e = 1000 μs. A total of 34 data points were acquired at the top of each spin echo with a dwell time of t_{dw} = 10 μs. The duration of each CPMG decay was 2 s and 2048 echoes were recorded. A recycle delay of t_{RD} = 30 s was included between each scan, and 64 repeat scans were summed. Two-dimensional T_1-T_2 correlations were obtained using the IR-CPMG sequence [28,32]. In ^{13}C measurements the T_1 recovery interval was varied logarithmically from $t_1 = 100$ μs to 25 s over 30 separate acquisitions. The CPMG echo time was fixed at $t_e = 1000$ μs, with all other parameters equal to those given above. A recycle delay of $t_{RD} = 30$ s was included between each scan, and 8 signal averages were performed.

The 90° and 180° rf pulse durations for ^{1}H measurements were $t_{90} = 6.7$ μs and $t_{180} = 12.1$ μs, respectively. In ^{1}H CPMG experiments the echo time was $t_e = 200$ μs and $t_e = 1000$ μs depending on the T_2 of the sample. A total of 9 time domain data points were acquired at the top of each spin echo with a dwell time of $t_{dw} = 1$ μs. A recycle delay of $t_{RD} = 15$ s was included between each scan, and 4 signal averages were performed. In the ^{1}H IR-CPMG experiments, the T_1 recovery interval was varied logarithmically from $t_1 = 16.60$ μs to 3 s over 40 separate acquisitions. The CPMG echo time was fixed at $t_e = 1000$ μs, with all other parameters equal to those given above. A recycle delay of $t_{RD} = 20$ s was included between each scan, and 2 repeat scans were summed.

2.3 MR instruments

For bulk sample measurements, a 4.7 T vertical bore superconducting magnet (Cryomagnetics, TN) was used with a homebuilt ^{13}C RF probe with a resonance frequency of 50.3 MHz for ^{13}C. For measurements on core plugs, ^{13}C measurements were acquired using a variable field magnet (MR Solutions, Guildford, Surrey, UK) at 3.1 T with a resonance frequency of 33.7 MHz for ^{13}C. The RF probe was a homemade birdcage. The magnet is permanently connected to a magnet power supply (Cryomagnetics, Inc., TN, US). GIT system software (Green Imaging Technologies, Inc., NB, Canada) was employed to execute CPMG and IR-CPMG measurements.

All ^{1}H MR measurements were performed on a 23.4 MHz MQC-R (Oxford Instruments Ltd, Oxford, UK) permanent magnet. The RF probe has 26 mm inner diameter, driven by a 250W internal RF amplifier.

2.4 Processing

An in-house MATLAB script was used to process the CPMG data. A Fast Laplace Inversion algorithm (Laplace Inversion Software, Schlumberger-Doll Research) written in MATLAB (MathWorks, Natick, MA) was used to produce the T_2 distributions. GIT system software was used to process IR-CPMG data.

2.5 Theory

^{13}C is an MR sensitive nucleus with a 1.1% natural abundance, gyromagnetic ratio (γ) that is four times lower than that of ^{1}H. ^{13}C measurements have low sensitivity compared to ^{1}H. However, since ^{13}C only exists in the oil phase, it is favourable for core analysis using MR. The variation of the ^{13}C signal intensity per volume or the signal intensity per mass of the crude oils is unknown. Knowing the range that these quantities differ or understanding the variation of these quantities with respect to oil properties such as density is helpful in saturation determinations. In routine MR analysis to determine saturations it is necessary to have reference samples to convert the signal to mass or volume. The above study can eliminate this requirement. This study aims to quantify the error introduced to saturation measurement using ^{13}C, if a generic oil sample is used as a reference sample.

3 Results and discussion

3.1 Bulk measurements on crude oils

In the following ^{13}C and ^{1}H MR results for different crude oils are presented.

3.1.1 ^{13}C and ^{1}H signal intensity measurements

Figure 2 shows the ^{13}C and ^{1}H signal intensity per mass and signal intensity per volume of various crude oils. There is a clear linear trend with R^2 of ~80-97%. This suggests that both ^{1}H and ^{13}C show the same behaviour in terms of signal per mass and signal per volume versus density.

For signal per volume plots, the slope is gentle suggesting a minor variation especially among oils with densities less than 0.85. ^{1}H and ^{13}C signal per volume of oil samples show a confidence of variation ~ 4% and ~ 5%, respectively. The value of the ^{13}C signal per volume falls within ± 5% error. This is of great benefit if a reference sample from the saturating oil is not available. This suggests that there is no need to have a reference sample of the saturating oil to calculate the oil saturation. However, it is important to note that our conclusion is based on the samples we have tested, which include oils from different continents and cover a wide range of densities. While our findings are robust for the tested samples, they may not be directly applicable to heavy oils with an API gravity lower than 10. Further research and testing with a broader range of heavy oil samples would be necessary to generalize this conclusion.

Signal per mass plots suggest that there is a strong linear trend between signal per mass and the density of the crude oils. This implies that by knowing only the density of the crude oil and using Fig. 2, the ^{13}C signal can be converted to the oil mass and volume accurately. However, it is important to note that we do not have a detailed scientific explanation for this observation. Providing such an explanation would require more complex characterizations of the oils and their components. Nevertheless, we believe the relationship is robust due to the diversity of our samples. The oils are sourced from different companies, across different continents, and exhibit a range of densities. This diversity suggests that the observed relationship is unlikely to be random or coincidental. Further studies with more comprehensive analyses are needed to fully understand the underlying mechanisms.

These results reveal that when there is no information of the crude oil, the approach using signal per volume of the crude oil is preferred over the signal per mass of the samples. Also, since both signal per volume and signal per mass have linear trends with density, knowing an approximate value of the density of the unknown oil would help greatly in determining volume and mass by both ^{1}H and ^{13}C MR measurements. This is the case in oilfield studies, in which there is knowledge of the approximate densities of the crude oils even during the exploration phase.

It should be noted that in core plugs there might be signal loss due to short relaxation times. This produces inevitable error which exists in all ^{1}H and ^{13}C MR measurements. Two approaches can be considered to avoid this signal loss (1) using short echo times in CMPG method and (2) using FID instead of CPMG. Both approaches try to avoid the delays when acquiring signals.

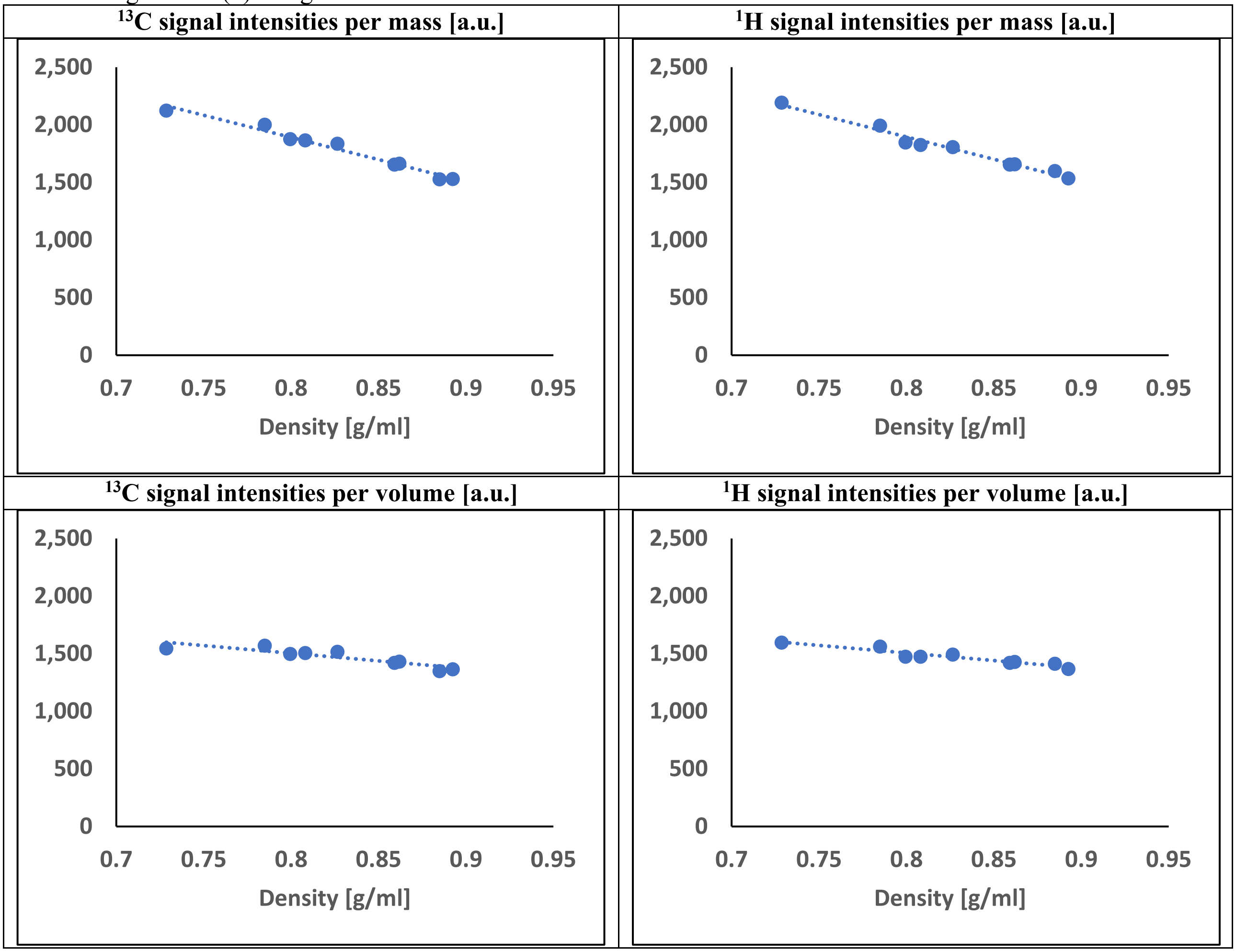

Fig. 2. ^{13}C and ^{1}H signal intensities per mass and signal intensities per volume for different crude oils. Signal intensities are in arbitrary unit [a.u.]. The trendline in ^{13}C signal intensity per mass vs. density has an R^2 of 97%, and the signal intensity per volume has an R^2 of 80%. The trendline in ^{1}H signal intensity per mass vs. density has an R^2 of 98%, and the signal intensity per volume has a R^2 of 90%. The coefficient of variation for ^{13}C signal intensity per mass and signal intensity per volume were 12% and 5.5% respectively. The coefficient of variation for ^{1}H signal intensity per mass and signal intensity per volume were 11% and 4.7% respectively.

3.1.2 ^{13}C and ^{1}H T_1-T_2 measurements

Figure 3 shows the ^{13}C and ^{1}H T_1-T_2 for the oils which displays a clear variation between different oils. Oil1 (Decane) shows the simplest characteristic of a single peak, while crude oils show distributions in both T_1 and T_2. The ^{1}H and ^{13}C T_1-T_2 relaxation correlation for some of the crude oils shows similar trends and have similar ranges. Decane shows a significantly different behavior between ^{1}H and ^{13}C MR relaxations times. This suggests further analysis to understand the components existing in those specific oils to explore the main dominant relaxation mechanisms.

Oil		**^{13}C T_1-T_2**		**^{1}H T_1-T_2**
Oil1	**T_{1LM}=4.82 s** **T_{2LM}=3.69 s** **T_1/T_2=1.3**	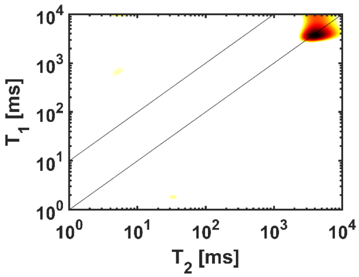	**T_{1LM}=1781 ms** **T_{2LM}=1770 ms** **T_1/T_2=1.0**	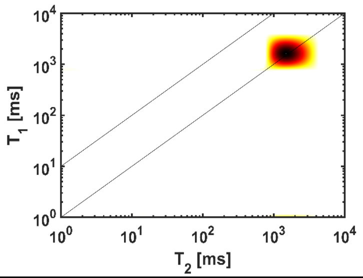
Oil2	**T_{1LM}=438 ms** **T_{2LM}=185 ms** **T_1/T_2=2.3**	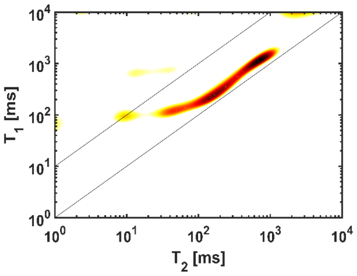	**T_{1LM}=127 ms** **T_{2LM}=70 ms** **T_1/T_2=1.8**	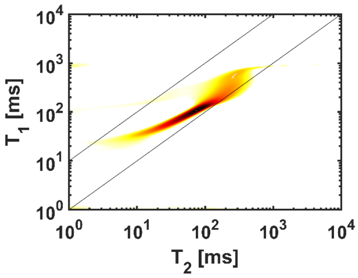
Oil3	**T_{1LM}=761 ms** **T_{2LM}=449 ms** **T_1/T_2=1.7**	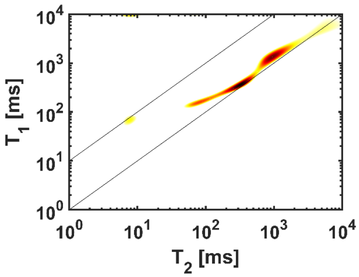	**T_{1LM}=295 ms** **T_{2LM}=202 ms** **T_1/T_2=1.5**	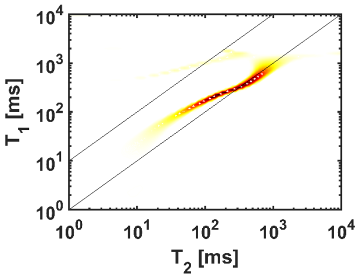
Oil4	**T_{1LM}=326 ms** **T_{2LM}=23.3 ms** **T_1/T_2=14**	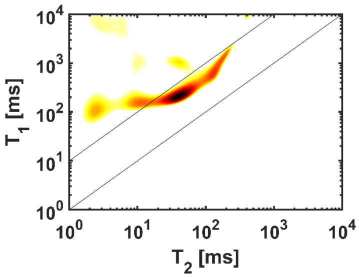	**T_{1LM}=80 ms** **T_{2LM}=12 ms** **T_1/T_2=6.8**	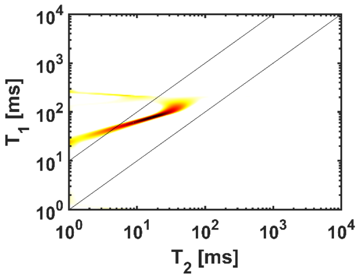
Oil5	**T_{1LM}=1.38 s** **T_{2LM}=1.02 s** **T_1/T_2=1.4**	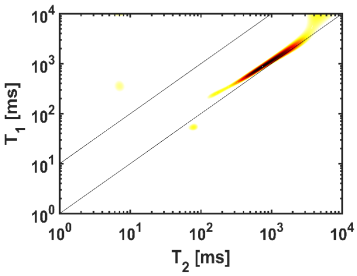	**T_{1LM}=638 ms** **T_{2LM}=595 ms** **T_1/T_2=1.1**	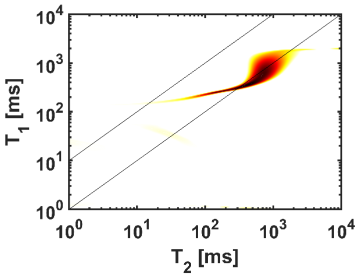
Oil6	**T_{1LM}=466 ms** **T_{2LM}=70.2 ms** **T_1/T_2=6.6**	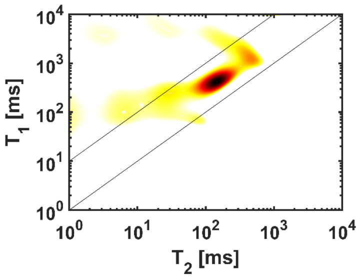	**T_{1LM}=124 ms** **T_{2LM}=28 ms** **T_1/T_2=4.4**	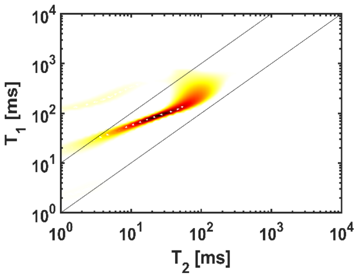

Oil7	**$T_{1\mathrm{LM}}$=536 ms** **$T_{2\mathrm{LM}}$=67.5 ms** **T_1/T_2=7.9**	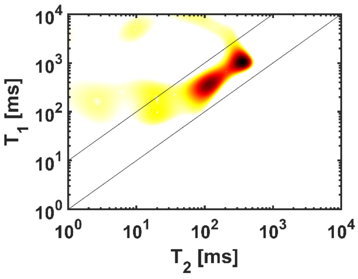	**$T_{1\mathrm{LM}}$=125 ms** **$T_{2\mathrm{LM}}$=23 ms** **T_1/T_2=5.4**	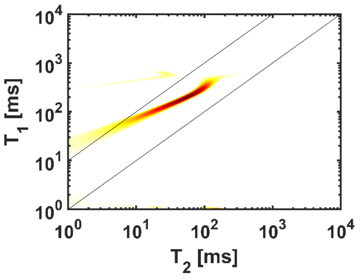
Oil8	**$T_{1\mathrm{LM}}$=1.52 s** **$T_{2\mathrm{LM}}$=1.11 s** **T_1/T_2=1.4**	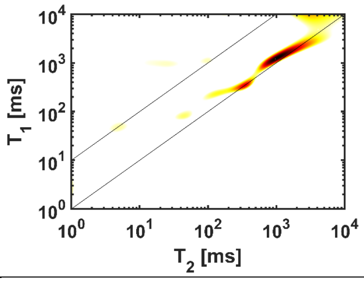	**$T_{1\mathrm{LM}}$=616 ms** **$T_{2\mathrm{LM}}$=527 ms** **T_1/T_2=1.2**	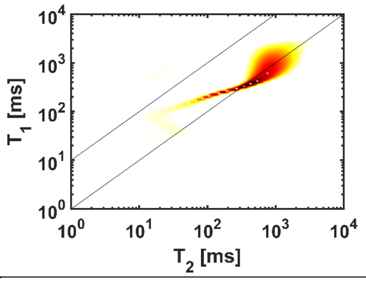
Oil9	**$T_{1\mathrm{LM}}$=712 ms** **$T_{2\mathrm{LM}}$=555 ms** **T_1/T_2=1.3**	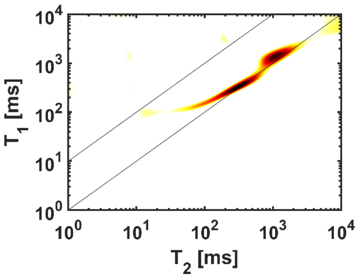	**$T_{1\mathrm{LM}}$=365 ms** **$T_{2\mathrm{LM}}$=328 ms** **T_1/T_2=1.1**	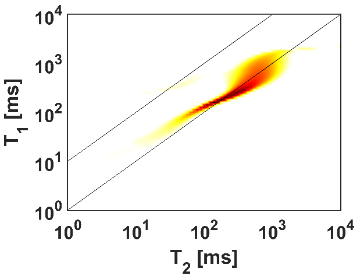

Fig. 3. ^{13}C and ^{1}H T_1-T_2 relaxation correlation for the crude oils. The two diagonal lines correspond to the T_1/T_2 of 1 and 10 respectively.

The analysis of the $T_{1\mathrm{LM}}$, $T_{2\mathrm{LM}}$ and $T_{1\mathrm{LM}}/T_{2\mathrm{LM}}$ from Figure 3 shows that there are similarities in trends between ^{1}H and ^{13}C relaxation times with respect to densities. Figure 4 compares the $T_{1\mathrm{LM}}/T_{2\mathrm{LM}}$ of ^{1}H and ^{13}C for the crude oil samples. As can be seen there is a clear trend with density. Figure 5 compares the ^{1}H and ^{13}C $T_{1\mathrm{LM}}$ and $T_{2\mathrm{LM}}$ for the crude oil samples. There is a linear relationship in logarithmic scale which shows a downwards trend of $T_{1\mathrm{LM}}$, $T_{2\mathrm{LM}}$ with respect to density of crude oil samples.

^{1}H	**^{13}C**
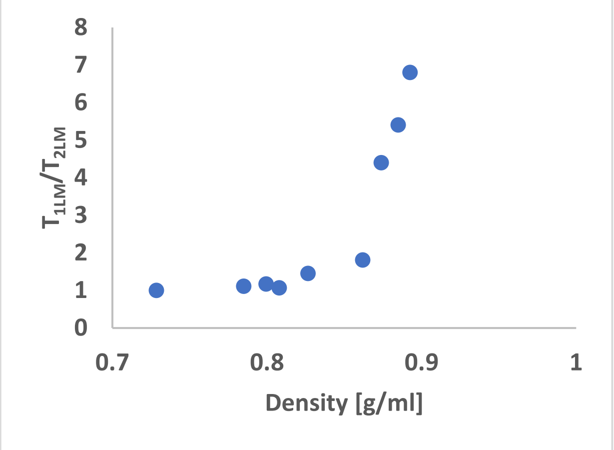	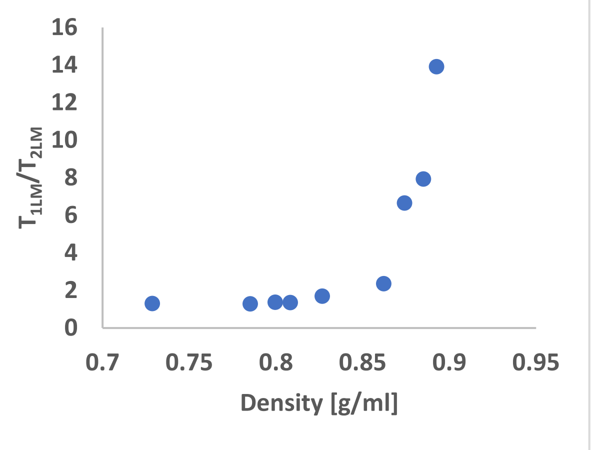

Fig. 4. ^{1}H $T_{1\mathrm{LM}}/T_{2\mathrm{LM}}$ (left) ^{13}C $T_{1\mathrm{LM}}/T_{2\mathrm{LM}}$ (right) and for different crude oil samples vs. density.

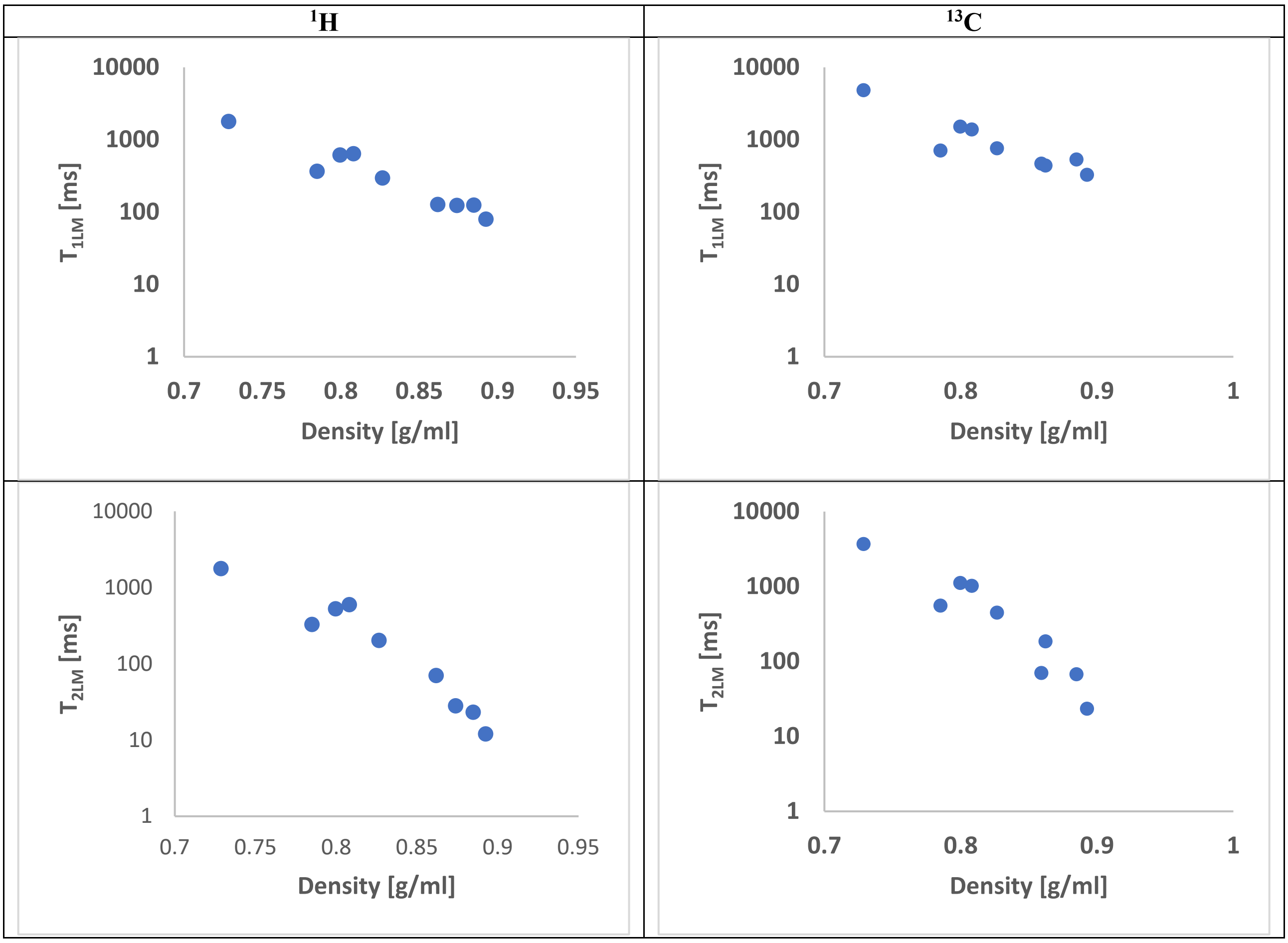

Fig. 5. ^{1}H $T_{1\mathrm{LM}}$ and $T_{2\mathrm{LM}}$ (left) and ^{13}C $T_{1\mathrm{LM}}$ and $T_{2\mathrm{LM}}$ (right) of crude oil samples.

3.2 Core plug

Figure 7 presents a comparison between the actual oil saturation of the core plugs and the oil saturation of the core plugs determined by converting ^{13}C signal intensities to volumes using signal per volume of dodecane. The results show that for this type of crude oil, using signal intensity per volume of other oils does not introduce a significant error in the oil saturation determination. This is consistent with our observations with bulk measurements, where the signal intensity per volume shows a gentle slope. This suggests that the signal intensity per volume is relatively insensitive to the type of crude oil.

It should be noted that error propagation can be minimized by obtaining the ^{13}C signal from the target sample with a high signal-to-noise ratio. In this way the error is introduced only during the conversion of the ^{13}C signal to volume using the mean signal per volume. Subsequently, this error is reduced during the conversion of volume to saturation units. If the signal per volume used for conversion has a coefficient of variation of 5%, then the relative error in saturation measurement will be a maximum of 5%. The term "maximum" is used because if the density of the oil used for calibration is close to the density of the saturating oil, then the relative error would be less than 5%. Moreover, the 5% relative error means that the error is 5% of the true value. If the true saturation is 30 saturation units (s.u.), the error would be 5% of 30, which is 0.05×30=1.5. So, the measured value could be anywhere between 28.5% and 31.5%.

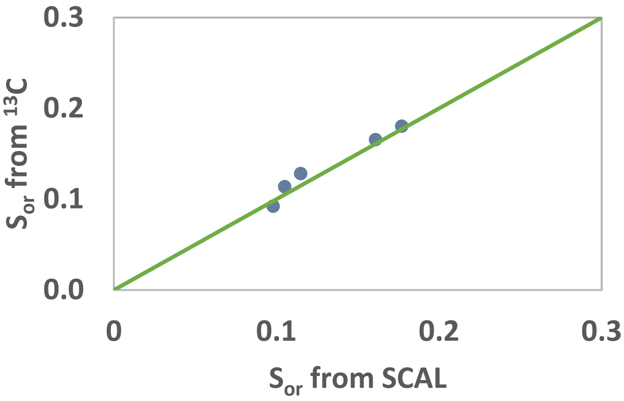

Fig. 6. Oil saturation obtained by ^{13}C MR measurement calibrated to signal intensity per volume of dodecane vs. oil saturation from SCAL.

4 Conclusions

Measurement of saturation in core plugs using MR is complicated by two factors. The ^{1}H signal originates from both water and oil phases. Therefore, MR signal needs to be resolved for oil and water. However, oil and water signals overlap in most practical cases. ^{13}C measurements only detects signal from oil phase. To accurately determine fluid saturation a reference sample is required. In this study we demonstrated the efficacy of employing a reference sample other than the actual reservoir fluid, and we reported on the error that this introduces in the saturation measurement. In this work, we utilized ^{13}C MR measurements as a valuable tool to investigate signal intensity of different crude oils with API ranging from 25 to 50. This showed that the ^{13}C signal intensity per volume and ^{13}C signal intensity per mass of different oils varies linearly with respect to density. Furthermore, ^{13}C T_1-T_2 and ^{1}H T_1-T_2 of these oils were compared to probe their relaxation times mechanisms.

Results showed that ^{13}C signal intensity per volume shows minimal variation. The coefficient of variation shows only 5% variation throughout the samples. This suggests using a different oil than the core plug saturating oil introduces at most 5% error in signal per volume. This can be largely reduced when an oil with the same density is used in the measurements. This is a step towards the goal of using a generic oil as the reference sample. The findings of our study have significant implications in exploratory phases of oil fields when limited data is available from the oil. To generalize the results presented in this study, we suggest testing a large number of crude oil samples with different properties such as density, gas content, impurity, etc.

^{13}C signal intensity per mass showed a strong linear relationship with density of the crude oil samples. This strong correlation can be used to calculate mass and volume of oil in the core plug when the oil density information is available. These results confirmed that ^{13}C MR can provide accurate saturation determinations even if there is limited information of the saturating oil.

Based on the current study's samples, using a completely different calibration sample introduces up to 5% error in the signal and volume calculations if no signal loss due to short components occurs in a core plug. This results in a maximum relative error of up to 5% in saturation measurements. However, it is important to note that these findings are based on the nine samples investigated. This conclusion should be validated with more samples, especially those with similar and different API gravity ranges, to ensure its generality.

^{1}H and ^{13}C T_1-T_2 relaxation correlations showed similar trends and ranges for most of the oils. This suggests that relaxation mechanisms for these samples might be the same. Further investigations and crude oil characterization are required which was beyond the scope of this study.

This work was supported by an NSERC Alliance award grant [ALLRP 571885–21] and an NSERC Discovery grant [2022-04003]. The authors thank TotalEnergies and Green Imaging Technologies for financial support.

References

1. J. Mitchell, J. Staniland, R. Chassagne, E.J. Fordham **94**, 683–706 (2012).
2. G. Asquith, D. Krygowski, S. Henderson, N. Hurley, Resistivity Logs, in: G. Asquith, D. Krygowski, S. Henderson, N. Hurley (Eds.), Basic well log analysis, American Association of Petroleum Geologists, (2004).
3. A. Awolayo, A. Ashqar, M. Uchida, A.A. Salahuddin, S.O. Olayiwola **7**, 637–657 (2017).
4. Y. Li, Z. Hu, C. Cai, X. Liu, X. Duan, J. Chang, Y. Li, Y. Mu, Q. Zhang, S. Zeng, J. Guo **128**, 105017 (2021).
5. J. Sam-Marcus, E. Enaworu, O.J. Rotimi, I. Seteyeobot **8**, 1009–1015 (2018).
6. M. Jamiolahmady, M. Sohrabi, M. Tafat (Eds.). SPE Europec/EAGE Annual Conference and Exhibition, SPE-107142-MS, (2007).
7. I. Mondal, K.H. Singh (Eds.). 11th Congress of the Balkan Geophysical Society, (2021).
8. API RP 40, Recommended practices for core analysis, American Petroleum Institute (API) Washington, DC, USA, (1998).
9. C. McPhee, J. Reed, I. Zubizarreta, Core analysis: A best practice guide, Elsevier, Amsterdam, 2015.
10. E.W. Dean, D.D. Stark **12**, 486–490 (1920). https://doi.org/10.1021/ie50125a025.
11. API Recommended Practice 40, Recommended Practices for Core Analysis, Second, American Petroleum Institute, 1220 L Street, N.W., Washington, (1998).
12. J. Mitchell, E.J. Forham, Rev. Sci. Instrum. **85** (2014).
13. R.L. Kleinberg **35**, 337–385 (1999).
14. J. Mitchell, A.M. Howe, A. Clarke **256**, 34–42 (2015).
15. P. Mitchell, L. Gromala, M. Siddiqui (Eds.). International Symposium of the Society of Core Analysts, SCA2017-063, (2017).
16. J. Mitchell, T.C. Chandrasekera, D.J. Holland, L.F. Gladden, E.J. Fordham **526**, 165–225 (2013).
17. W. Looyestijn (Ed.). SPE Middle East Oil & Gas Show and Conference, SPE 93624, 2006.
18. M.D. Hürlimann, Y.-Q. Song US Patent 8,362,767 B2, (2013).
19. Yi-Qiao Song, H. Cho, T. Hopper, A.E. Pomerantz, P.Z. Sun **128**, 52212 (2008).
20. G.R. Coates, L. Xiao, M.G. Prammer, NMR Logging Principles & Applications, Gulf Publishing Company, Halliburton Energy Services, Houston, (1999).
21. G.J. Hirasaki, S.-W. Lo, Y. Zhang **21**, 269–277 (2003).

22. N. Ansaribaranghar, M.S. Zamiri, L. Romero-Zerón, F. Marica, A. Ramírez Aguilera, D. Green, B. Nicot, B.J. Balcom (Eds.). International Symposium of the Society of Core Analysts, SCA2023-018, (2023).
23. N. Ansaribaranghar, M.S. Zamiri, L. Romero-Zerón, F. Marica, A. Ramírez Aguilera, D. Green, B. Nicot, B.J. Balcom (Eds.). International Symposium of the Society of Core Analysts, SCA2023-005, (2023).
24. Y.-Q. Song, L. Venkataramanan, M.D. Hürlimann, M. Flaum, P. Frulla, C. Straley, J. Magn. Reson. **154**, 261–268 (2002).
25. J. Mitchell, T.C. Chandrasekera, L.F. Gladden, Prog. Nucl. Magn. Reson. Spectrosc. **62**, 34–50 (2012).
26. K.M. Song, J. Mitchell, H. Jaffel, L.F. Gladden, J. Mater. Sci. **45**, 5282–5290 (2010).
27. S. Vashaee, M. Li, B. Newling, B. MacMillan, F. Marica, H.T. Kwak, J. Gao, A.M. Al-harbi, B.J. Balcom **287**, 113–122 (2018).